



Proceedings of ICACTCE'21

High School of Technology, Moulay Ismail University Meknes, Morocco, and

Faculty of Sciences and Techniques Mohammeda, Hassan II University, Morocco

March 24 – 26, 2021, Morocco

Editors: Mariyam Ouaisa, Mariya Ouaisa, Sarah El Himer, and Zakaria Boulouard

Research Article

Lattice Boltzmann Simulation of MHD Rayleigh-Bénard Natural Convection in a Cavity Filled With a Ferrofluid

Khalid Chtaibi^{*}, Mohammed Hasnaoui, Youssef Dahani and
Abdelkhalek Amahmid

LMFE, Department of Physics, Cadi Ayyad University, Faculty of Sciences Semlalia,
B.P. 2390, Marrakesh, Morocco

Abstract. In this study, we examine the effect of a uniform external magnetic field on Rayleigh-Bénard convection in a square cavity filled with a ferrofluid. Numerical simulations are based on the Lattice Boltzmann method. The effects of physical parameters, which are the Rayleigh number, the Hartmann number, and the angle of inclination of the magnetic field are studied. The results obtained are graphically illustrated and discussed for a volume fraction of four percent. These results show that the rate of heat transfer decreases by increasing the Hartmann number. For high Rayleigh number values, the maximum heat transfer rate was obtained for a specific Hartmann number when the Lorentz and buoyancy forces are perpendicular.

Keywords. Magnetohydrodynamics; Rayleigh-Bénard Convection; Ferrofluid $\text{Fe}_3\text{O}_4\text{-H}_2\text{O}$

PACS. 44.90.+c; 44.25.+f; 44.10.+I; 47.65.-d

Copyright © 2020 Khalid Chtaibi, Mohammed Hasnaoui, Youssef Dahani and Abdelkhalek Amahmid. *This is an open access article distributed under the Creative Commons Attribution License, which permits unrestricted use, distribution, and reproduction in any medium, provided the original work is properly cited.*

1. Introduction

Heat transfer generated by *Rayleigh-Bénard* (RB) convection in confined spaces has been the subject of several studies [11,17]. This interest is motivated by the involvement of such problems in various applications, such as reactor cooling, solar collectors, heat exchangers, and crystal

^{*}Corresponding author: khalid.chtaibi@edu.uca.ac.ma

growth, etc. [1]. RB configurations constitute a category apart of problems that require critical thresholds to trigger the confined fluids' movements. The presence of an additional force (e.g. Lorentz force) to the buoyancy one may have a considerable effect (depending on its intensity) on the threshold values in such problems. On another side, the low thermal conductivity values of conventional basic fluids such as water, ethylene glycol, oil, etc., reduce the performances of the systems involving these fluids for cooling purposes. In 1995, Choi [4] proposed to add nano-sized solid particles suspended in water (base fluid) to form a homogeneous mixture called nanofluid. Their results show an improvement of heat transfer in the presence of these nanoparticles.

The literature review shows that numerous studies have been devoted to the analysis of convective heat transfer by natural convection in systems containing nanofluids. For instance, Khanafer *et al.* [9] used the volume control method to study the heat transfer in a differentially heated square cavity using the nanofluid copper-water. They concluded that the increase of the volume fraction of nanoparticles has a positive effect on heat transfer. Ho *et al.* [8] carried out an experimental investigation on natural convection in three square enclosures of different sizes, confining the nanofluid $\text{Al}_2\text{O}_3\text{-H}_2\text{O}$. They have examined the combined effects of the Rayleigh number and the volume fraction of nanoparticles in these configurations. Recently, the impact of *magnetohydrodynamic forces* (MHD) on flow characteristics and heat transfer of nanofluids, generated by natural convection, has been widely studied. The problem of natural convection in a square cavity confining the nanofluid $\text{Al}_2\text{O}_3\text{-H}_2\text{O}$ and subjected to an external magnetic field was investigated numerically by Mahmoudi *et al.* [10]. In this study, the simulation tool was based on the lattice-Boltzmann method. Rahimpour and Moraveji [13] carried out a numerical study by modeling natural convection heat transfer in a C-shaped inclined cavity filled with the ferrofluid $\text{Fe}_3\text{O}_4\text{-H}_2\text{O}$ under the effect of a magnetic field. The results presented show that heat transfer decreases by increasing the magnetic field strength characterized by the Hartmann number. This trend confirms the slowing down of conductive fluid flows generated by the increase of the magnetic field. On another side, magnetic nanofluids (ferrofluid) have an inherent advantage compared to non-magnetic nanofluids, resulting from the fact that, for the formers, the magnetic field can be used to control thermomagnetic convection. Furthermore, earlier experimental studies have shown that the thermal conductivity of the ferrofluid may be improved by about 300% for a certain orientation of the magnetic field, which is about six times higher than that of non-magnetic nanofluids [12, 15].

The aim of this study is to examine the impact of a magnetic field inclination on the flow characteristics and heat transfer in a Rayleigh-Bénard square cavity filled with the ferrofluid $\text{Fe}_3\text{O}_4\text{-H}_2\text{O}$.

2. Mathematical Formulation

2.1 Description of the Physical Problem

The studied two-dimensional physical model is shown schematically in Figure 1. It is a square cavity ($L \times L$) thermally insulated from its vertical sides, heated from below and cooled from

above. The cavity is filled with the ferrofluid $\text{Fe}_3\text{O}_4\text{-H}_2\text{O}$, assumed Newtonian and subjected to the action of a uniform and inclined external magnetic field. Moreover, the flow is laminar, and all the thermo-physical properties of the ferrofluid are considered constant, except the density in the buoyancy term, which obeys the Boussinesq approximation.

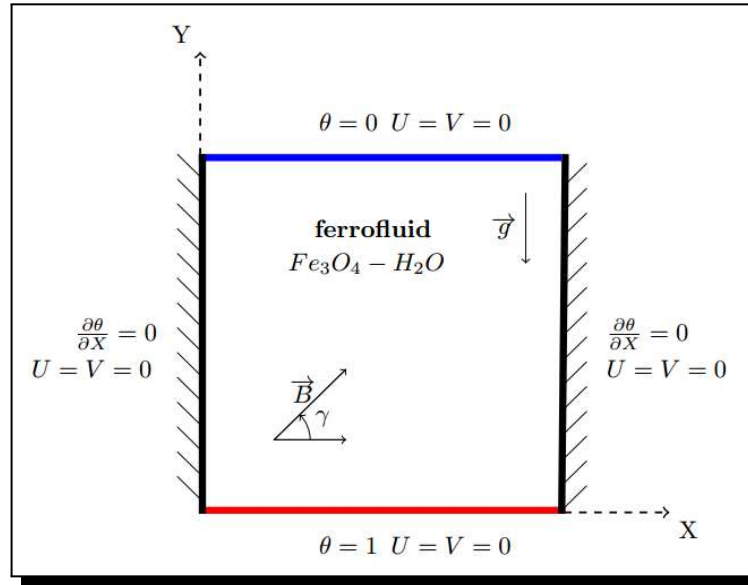


Figure 1. Schematic of the studied configuration

2.2 Lattice Boltzmann method

The method used in this study is the *Lattice Boltzmann Method* (LBM), preferred by many authors over conventional methods for objective reasons. Its main advantages lie in its simplicity, its stability, and its ease of adaptation to face the complex problems of thermal convection.

After linearizing the collision term by the *Bhatnagar-Gross-Krook* (BGK) approximation [2], two independent distribution functions are used to solve the momentum (2.1) and energy equations (2.2). The numerical simulation is achieved in two steps; the collision between the fluid particles (the term on the right side of eq. (2.1)) and the streaming between these particles (the first term on the left side of eq. (2.1)) according to the D2Q9 model (Figure 2). The lattice Boltzmann equation in the presence of an external force can be written for the flow and temperature fields as follows:

$$f_k(\vec{r} + e_k \Delta t, t + \Delta t) - f_k(\vec{r}, t) = \frac{\Delta t}{\tau_v} (f_k^{eq}(\vec{r}, t) - f_k(\vec{r}, t)) + \Delta t F_k, \quad (2.1)$$

$$g_k(\vec{r} + e_k \Delta t, t + \Delta t) - g_k(\vec{r}, t) = \frac{\Delta t}{\tau_\alpha} (g_k^{eq}(\vec{r}, t) - g_k(\vec{r}, t)), \quad (2.2)$$

where (\vec{r}, t) is the instantaneous position of the fluid particle. e_k is the discrete velocity in the direction k . The parameters $\tau_v = 3\nu + 1/2$ and $\tau_\alpha = 3\alpha + 1/2$ are respectively the relaxation time coefficients of the momentum and energy equations and F_k is the external force at the lattice scale.

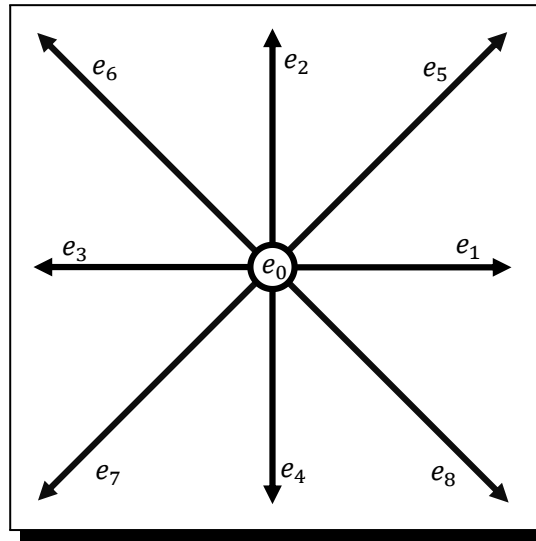


Figure 2. Discrete speeds of the D2Q9 model

The quantities f_k^{eq} and g_k^{eq} are respectively the equilibrium distribution functions for velocity and temperature fields, defined by eqs. (2.3) and (2.4).

$$f_k^{eq} = \omega_k \rho \left(1 + 3\vec{e}_k \vec{u} + \frac{9}{2}(\vec{e}_k \vec{u})^2 - \frac{3}{2}(\vec{u})^2 \right), \tag{2.3}$$

$$g_k^{eq} = \omega_k \theta (1 + 3\vec{e}_k \vec{u}), \tag{2.4}$$

where ρ is the fluid density at the lattice scale and ω_k is the weighting factor. For the D2Q9 model, e_k and ω_k are defined as follows:

$$e_k = \begin{cases} (0, 0), & \text{for } k = 0, \\ (\cos(\pi(k-1)/2), \sin(\pi(k-1)/2)), & \text{for } k = 1-4, \\ \sqrt{2}(\cos(\pi(k-9/2)/2), \sin(\pi(k-9/2)/2)), & \text{for } k = 5-8, \end{cases} \tag{2.5}$$

$$\omega_k = \begin{cases} 4/9, & \text{for } k = 0, \\ 1/9, & \text{for } k = 1-4, \\ 1/36, & \text{for } k = 5-8. \end{cases} \tag{2.6}$$

The external force term, F_k in eq. (2.1), is composed by two forces (the buoyancy and magnetic forces) evaluated as:

$$\left. \begin{aligned} F_x &= A(\sin(\gamma)\cos(\gamma)v - u\sin^2(\gamma)), \\ F_y &= g\beta(\theta - \theta_m) + A(\sin(\gamma)\cos(\gamma)u - v\cos^2(\gamma)), \\ F_k &= 3\omega_k \rho (e_{kx}F_x + e_{ky}F_y) \end{aligned} \right\} \tag{2.7}$$

where $A = Ha^2 \partial/L^2$, $Ha = LB_0 \sqrt{\sigma_f/\mu_f}$ is the Hartmann number and γ is the inclination of the magnetic field relative to the horizontal axis.

The macroscopic quantities ρ , u , v , and θ are calculated using the following expressions:

$$\left. \begin{aligned} \rho &= \sum f_k, & u &= \frac{1}{\rho} \sum f_k e_{kx}, \\ v &= \frac{1}{\rho} \sum f_k e_{ky}, & \theta &= \sum g_k. \end{aligned} \right\} \tag{2.8}$$

2.3 Boundary Conditions

For velocity: the rigid walls that delimit the physical domain are motionless. At the lattice scale, the distribution functions pointing outside the physical domain are known after streaming. The distribution functions pointing inside the physical domain at the rigid walls are calculated using bounce-back boundary conditions.

For temperature: At the adiabatic vertical walls, temperatures are determined by assuming that the first derivative of each distribution function g is null. For the isothermal walls, the distribution functions are defined as follows:

$$\left. \begin{aligned} g_4 &= \theta_c(\omega_4 + \omega_2) - g_2 \\ g_7 &= \theta_c(\omega_7 + \omega_5) - g_5 \\ g_8 &= \theta_c(\omega_8 + \omega_6) - g_6 \end{aligned} \right\} \text{ (Top wall)} \quad \left. \vphantom{\begin{aligned} g_4 &= \theta_c(\omega_4 + \omega_2) - g_2 \\ g_7 &= \theta_c(\omega_7 + \omega_5) - g_5 \\ g_8 &= \theta_c(\omega_8 + \omega_6) - g_6 \end{aligned}} \right\} \quad (2.9)$$

$$\left. \begin{aligned} g_2 &= \theta_h(\omega_2 + \omega_4) - g_4 \\ g_5 &= \theta_h(\omega_5 + \omega_7) - g_7 \\ g_6 &= \theta_h(\omega_6 + \omega_8) - g_8 \end{aligned} \right\} \text{ (Bottom wall)}$$

2.4 Lattice Boltzmann for Ferrofluid

The LBM is very suitable to simulate the convective heat transfer of ferrofluids (magnetic nanofluids). The latter behave differently at the mesoscopic scale compared to pure fluids. In the present study, the hypotheses of nanoparticles uniformly dispersed in the base fluid (homogeneous mixture) and in thermal equilibrium with the latter are adopted. Thermo-physical properties of ferrofluid [6], listed in Table 1 (density (ρ_{ff}/ρ_f) , specific heat $((\rho c_p)_{ff}/(\rho c_p)_f)$, thermal expansion (β_{ff}/β_f) , dynamic viscosity (μ_{ff}/μ_f) , thermal conductivity (k_{ff}/k_f) , and electrical conductivity (σ_{ff}/σ_f)) are evaluated using correlations that are taken into account in the governing equations [5].

$$\left. \begin{aligned} \rho_{ff} &= (1 - \varphi)\rho_f + \varphi\rho_s \\ (\rho c_p)_{ff} &= (1 - \varphi)(\rho c_p)_f + \varphi(\rho c_p)_s \\ \beta_{ff} &= (1 - \varphi)\beta_f + \varphi\beta_s \end{aligned} \right\} \quad (2.10)$$

The dynamic viscosity is expressed by the Brinkman model [3]:

$$\frac{\mu_{ff}}{\mu_f} = \frac{1}{(1 - \varphi)^{2.5}}. \quad (2.11)$$

Thermal conductivity is evaluated by the Hamilton and Crosser model [7]:

$$\frac{k_{ff}}{k_f} = \frac{k_s + 2k_f - \varphi(k_f - k_s)}{k_s + 2k_f + \varphi(k_f - k_s)}. \quad (2.12)$$

The Prandtl and Rayleigh numbers, which are among the parameters of the problem, are defined as follows:

$$Pr = \nu_f/\alpha_f \quad \text{and} \quad Ra = g\beta\Delta TL^3/\nu_f\alpha_f. \quad (2.13)$$

The local Nusselt number at the hot wall is evaluated as:

$$Nu_{loc} = -\frac{k_{ff}}{k_f} \frac{\partial\theta}{\partial Y} \Big|_{Y=0}. \quad (2.14)$$

Whereas the average Nusselt number is defined by:

$$Nu_m = \int_0^1 Nu_{loc} dX. \quad (2.15)$$

Table 1. Thermo-physical properties of water and nanoparticles [6]

	Pure water	Fe ₃ O ₄
Pr	6.200	
$\rho(\text{Kg/m}^3)$	997.100	5200.00
$C_p(\text{J/Kg K})$	4179.000	670.00
$K(\text{W/m K})$	0.613	6.00
$\beta \times 10^5(\text{K}^{-1})$	21.000	1.30
$\sigma(\text{m}\Omega)^{-1}$	0.050	25000.00

3. Numerical Validation of the LBM Code

The present numerical code was firstly validated against different works published in the literature in the case of natural convection in a square cavity heated from below, cooled from above (Rayleigh-Bénard configuration), and filled with air ($Pr = 0.71$). The comparative results presented in Table 2, in terms of Nusselt numbers for various Rayleigh numbers, show that the LBM code reproduces the results obtained by Ouertatani *et al.* [11], Turan *et al.* [16], and Xu *et al.* [17] with a maximum deviation of 0.57%. In addition, the code was validated qualitatively in the presence of an inclined magnetic field against the results published by Sathiyamoorthy and Chamkha [14]. The results presented in Figure 3 in the case of a square cavity filled with the gallium and obtained with $Ra = 10^5$, $Ha = 50$, $Pr = 0.025$, and a magnetic field tilted with an angle of 90° , show an excellent qualitative agreement. Finally, the sensitivity of the results with respect to the grid was carried out using the grids 120×120 , 160×160 , 240×240 and 320×320 . The results obtained for $Ra = 10^5$, $\varphi = 4\%$, $Ha = 50$ and a convergence condition of 10^{-8} (not presented here) have shown that the uniform grid 160×160 was enough to carry out this study.

Table 2. Comparison of Nusselt number of our code and the results of Ouertatani *et al.* [11], Turan *et al.* [16], and Xu *et al.* [17]

Ra	Our code	Ref. [11]	Ref. [16]	Ref. [17]	Max deviation
10^4	2.1594	2.1581	2.154	2.1581	0.25%
10^5	3.9174	3.9103	3.907	3.9102	0.27%
10^6	6.3447	6.309	3.363	...	0.57%

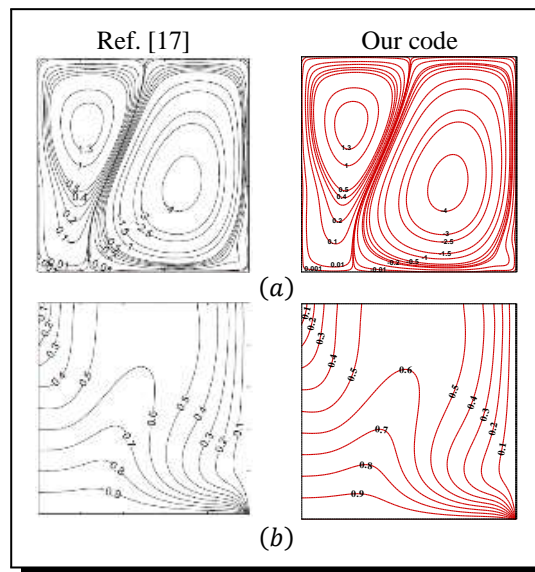


Figure 3. Validation in terms of streamlines (a), and isotherms (b), against the results presented in Ref. [14] (left), for $Ra = 10^5$, $Ha = 50$, $Pr = 0.025$ and $\gamma = 90^\circ$

4. Results and Discussion

The present study focuses on the impact of an inclined uniform magnetic field on heat transfer and ferrofluid flow for two values of Rayleigh number ($Ra = 10^4$ and 10^5), various values of Hartmann number ($Ha = 0, 25$ and 50), and an inclination γ of the magnetic field varying between 0° and 135° with an increment of 45° . The volume fraction of nanoparticles is fixed at $\varphi = 4\%$.

4.1 Effect of Hartmann Number for $\gamma = 0^\circ$

The Hartmann number effect on the ferrofluid $Fe_3O_4-H_2O$ is illustrated in Figures 4 and 5 for the streamlines and isotherms, respectively. For a given Rayleigh number, the increase of Ha leads to significant qualitative and quantitative changes in the flow intensity and structure in the convective regime in the presence of the magnetic field. In fact, Figure 4 shows that the increase of the Hartmann number brings the fluid flow back to the rest state from a critical Hartmann number ($Ha_c = 19$) for $Ra = 10^4$, and reduces considerably its intensity for $Ra = 10^5$. For the latter value of Ra , for which the convection survives in the whole range of Ha , the most important qualitative changes are observed in the central region of the cavity. In fact, the central cells are horizontal for $Ha = 0$, take an oval shape for $Ha = 25$ and straighten up to approach the vertical shape for $Ha = 50$. Moreover, the increase of Ha causes a disappearance of the secondary cells without modifying too much the trajectories of the particles on the peripheral lines, which remain practically parallel to the walls apart from the effect of the corners. Overall, the effect of the Lorentz force is opposite to that of the buoyancy force and the higher the Rayleigh number the higher the Hartmann number required to bring the ferrofluid flow back to a static state. Due to the strong coupling between the velocity and temperature

fields, the qualitative and quantitative effects on the temperature distribution inside the cavity, accompanying the increase of the Hartmann number are important as it can be seen in Figure 5. Indeed, in the presence of the magnetic field, the distortions of the isotherms observed for $Ra = 10^5$ are more and more attenuated in the central region of the cavity and the thermal gradients at the level of the active walls are more and more weakened by incrementing Ha .

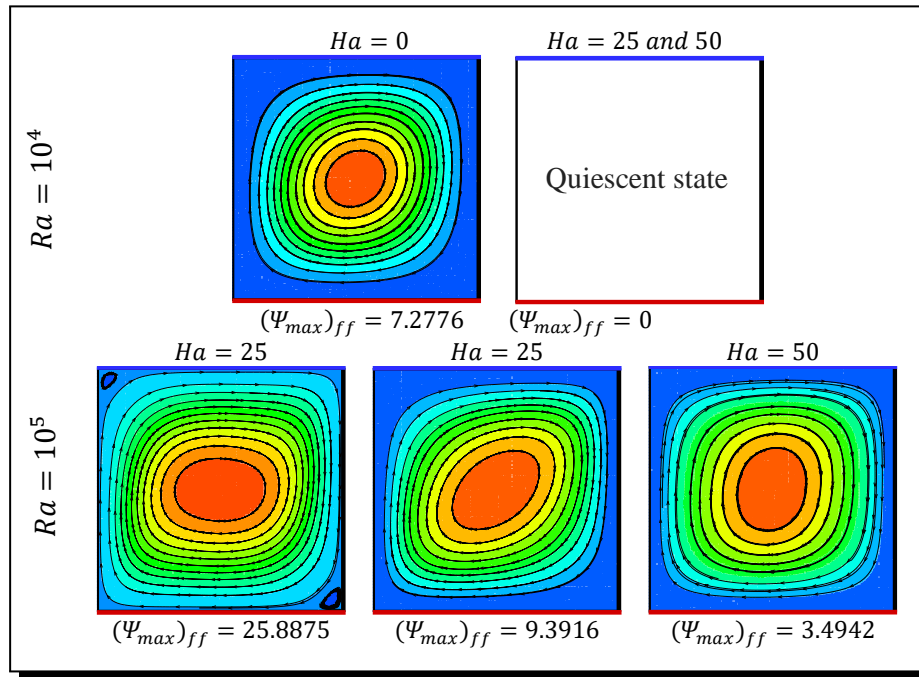


Figure 4. Streamlines for $\varphi = 4\%$ and different values of Ra and Ha

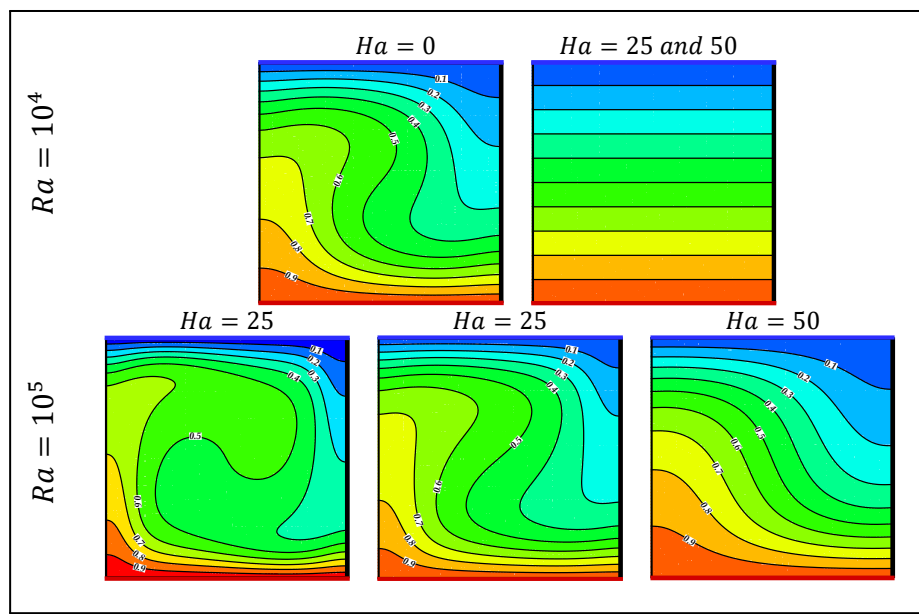


Figure 5. Isotherms for $\varphi = 4\%$ and different values of Ra and Ha

4.2 Effect of the Inclination Angle of the Magnetic Field

For large values of the Hartmann number, just above the threshold value $Ha = 19$, the ferrofluid flow becomes purely conductive at $Ra = 10^4$ since the Lorentz force overcomes the buoyancy one. To clearly demonstrate the effect of the inclination angle of the magnetic field, the value of Ra was set at 10^5 . The effect of the inclination angle of the magnetic field is illustrated in Figure 6a for $Ra = 10^5$ and $Ha = 50$. It is to underline that the flow structure remains monocellular for $Ha = 25$ while varying the inclination of the magnetic field in its range but the intensity of the flow and the shape of the central cells are affected by varying the parameter γ (results not presented). However, for $Ha = 50$ the transformations undergone by the flow structure and resulting from the variation of the inclinations are spectacular. In fact, by increasing the inclination γ from 0° to 45° , the flow switches from a monocellular structure to a multicellular one consisting of three cells inclined parallel to a diagonal of the cavity, and presenting a symmetry with respect to the latter. The inclination 90° straightens the three cells that take the vertical position while preserving the flow symmetry with respect to the vertical median. For $\gamma = 135^\circ$, the flow structure becomes mainly unicellular again with the positive central cell, observed for $\gamma = 45^\circ$ and 90° , totally dominating the flow and its axis of symmetry is the second diagonal of the cavity. In this structure, the two negative cells are reduced to two small vortices, one located at the upper right corner of the cavity and the other at its lower left corner. These important transformations of the flow structure, resulting from the change of the Lorentz force direction (that is perpendicular to the magnetic field vector), show that the direction of the imposed magnetic field is an important parameter that may play a role and should not be ignored.

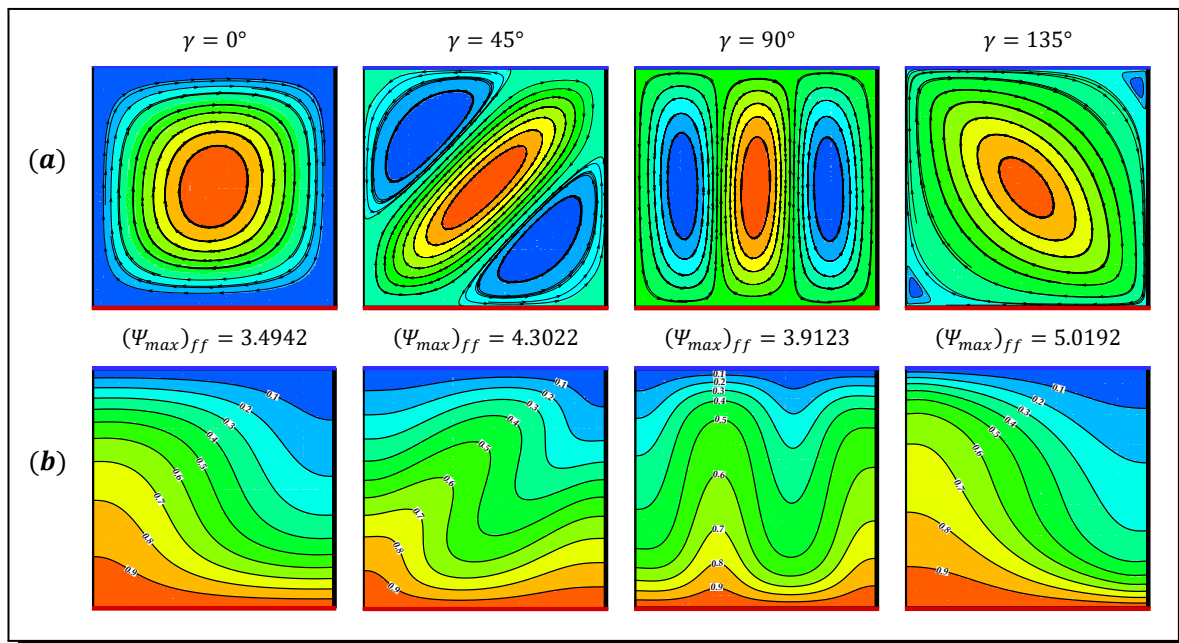


Figure 6. Streamlines (a) and isotherms (b) for $Ra = 10^5$, $\varphi = 4\%$, $Ha = 50$ and different values of γ

Regarding the thermal behavior shown in Figure 6b in terms of isotherms, it can be observed that the temperature distribution within the cavity is very much affected by the nature of the corresponding flow (number of cells, their intensities, their orientations, their interactions with the active walls, etc.). More specifically, for $Ha = 50$ the distribution of the temperature field presents an aspect more or less complex depending if the flow structure is multicellular or unicellular, which is a consequence of the strong coupling between velocity and temperature in thermal natural convection.

4.3 Heat Transfer

For the evaluation of the impact of the magnetic field orientation on the average heat transfer, Figure 7 exemplifies the variations of Nu_m versus γ for $Ra = 10^5$, $\varphi = 4\%$ and different values of the Hartmann number. The first remark, expected due to the damping role of the magnetic field, is the negative impact of Ha on heat transfer for all inclinations γ . In addition, it is obvious that Nu_m remains insensible to the variations of γ for $Ha = 0$ due to the absence of the magnetic field. Nevertheless, for $Ha = 50$ the magnetic field orientation has a non-negligible effect on the average heat transfer, and leads to irregular variations in the mean Nusselt number by varying γ . These irregularities are attributed to the changes in thermal gradients in the walls, accompanying the changes undergone by the convective structures. Overall, for a given inclination of the magnetic field, the average heat transfer decreases drastically by increasing the Hartmann number.

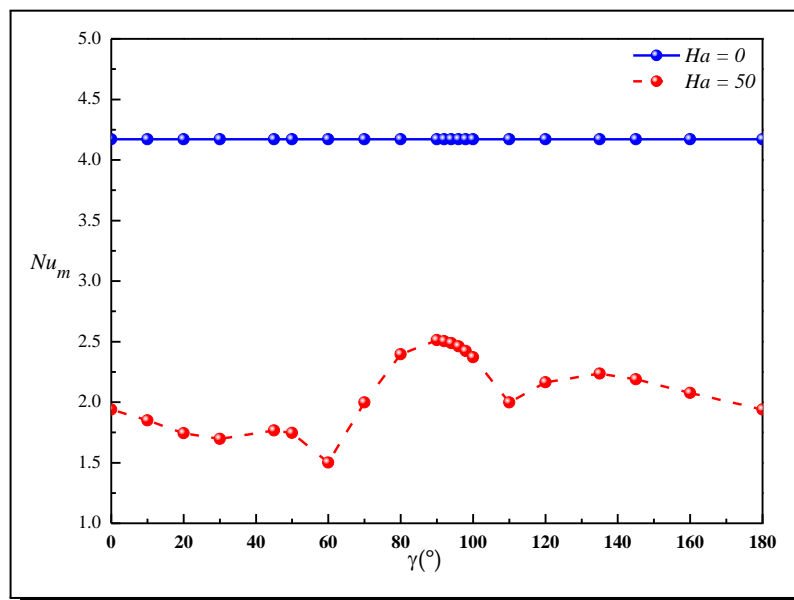


Figure 7. Variations of the average Nusselt number vs. the inclination of the magnetic field for $Ra = 10^5$

5. Conclusion

The present study reports preliminary results obtained based on numerical simulations of natural convection in a Rayleigh-Bénard-type square cavity filled with a ferrofluid under

the effect of an external magnetic field. The equations describing the physical problem were solved using the lattice Boltzmann method. The results of this study show that the increase of the Hartmann number brought back the ferrofluid flow to the rest state from some threshold value that depends on Ra . Moreover, in addition to the magnetic field intensity, its orientation is also a parameter that plays a non-negligible role. Finally, the study should be treated in more depth to elucidate the hidden aspects of this problem.

Competing Interests

The authors declare that they have no competing interests.

Authors' Contributions

All the authors contributed significantly in writing this article. The authors read and approved the final manuscript.

References

- [1] A. Baïri, E. Zarco-Pernia and J.M. García De María, A review on natural convection in enclosures for engineering applications, the particular case of the parallelogrammic diode cavity, *Applied Thermal Engineering* **63** (2014), 304 – 322, DOI: 10.1016/j.applthermaleng.2013.10.065.
- [2] A.P.L. Bhatnagar, E.P. Gross and M. Krook, A model for collision processes in gases. I. Small amplitude processes in charged and neutral one-component systems, *Physical Review* **94** (1954), 511 – 525, DOI: 10.1103/PhysRev.94.511.
- [3] H.C. Brinkman, The viscosity of concentrated suspensions and solutions, *The Journal Chemical Physics* **20** (1952), 571, DOI: 10.1063/1.1700493.
- [4] S.U.S. Choi and J.A. Eastman, *Enhancing Thermal Conductivity of Fluids With Nanoparticles*, ASME-Publications-Fed 231 (1995).
- [5] A.S. Dogonchi and Hashim, Heat transfer by natural convection of Fe_3O_4 -water nanofluid in an annulus between a wavy circular cylinder and a rhombus, *International Journal of Heat and Mass Transfer* **130** (2019), 320 – 332, DOI: 10.1016/j.ijheatmasstransfer.2018.10.086.
- [6] O. Ghaffarpasand, Numerical study of MHD natural convection inside a sinusoidally heated lid-driven cavity filled with Fe_3O_4 -water nanofluid in the presence of Joule heating, *Applied Mathematical Modelling* **40** (2016), 9165 – 9182, DOI: 10.1016/j.apm.2016.05.038.
- [7] R.L. Hamilton and O.K. Crosser, Thermal conductivity of heterogeneous two-component systems, *Industrial and Engineering Chemistry Fundamentals* **1** (1962), 187 – 191, DOI: 10.1021/i160003a005.
- [8] C.J. Ho, W.K. Liu, Y.S. Chang and C.C. Lin, Natural convection heat transfer of alumina-water nanofluid in vertical square enclosures: an experimental study, *International Journal of Thermal Sciences* **49** (2010), 1345 – 1353, DOI: 10.1016/j.ijthermalsci.2010.02.013.
- [9] K. Khanafer, K. Vafai and M. Lightstone, Buoyancy-driven heat transfer enhancement in a two-dimensional enclosure utilizing nanofluids, *International Journal of Heat and Mass Transfer* **46** (2003), 3639 – 3653, DOI: 10.1016/S0017-9310(03)00156-X.

- [10] A. Mahmoudi, I. Mejri, M.A. Abbassi and A. Omri, Lattice Boltzmann simulation of MHD natural convection in a nanofluid-filled cavity with linear temperature distribution, *Powder Technology* **256** (2014), 257 – 271, DOI: 10.1016/j.powtec.2014.02.032.
- [11] N. Ouertatani, N.B. Cheikh, B.B. Beya and T. Lili, Numerical simulation of two-dimensional Rayleigh-Bénard convection in an enclosure, *Comptes Rendus Mécanique* **336** (2008), 464 – 470, DOI: 10.1016/j.crme.2008.02.004.
- [12] J. Philip, P.D. Shima and B. Raj, Enhancement of thermal conductivity in magnetite based nanofluid due to chainlike structures, *Applied Physics Letters* **91** (2007), 203108, DOI: 10.1063/1.2812699.
- [13] N. Rahimpour and M.K. Moraveji, Free convection of water — Fe₃O₄ nanofluid in an inclined cavity subjected to a magnetic field: CFD modeling, sensitivity analysis, *Advanced Powder Technology* **28** (2017), 1573 – 1584, DOI: 10.1016/j.appt.2017.03.029.
- [14] M. Sathiyamoorthy and A. Chamkha, Effect of magnetic field on natural convection flow in a liquid gallium filled square cavity for linearly heated side wall(s), *International Journal of Thermal Sciences* **49** (2010), 1856 – 1865, DOI: 10.1016/j.ijthermalsci.2010.04.014.
- [15] P.D. Shima, J. Philip and B. Raj, Role of microconvection induced by Brownian motion of nanoparticles in the enhanced thermal conductivity of stable nanofluids, *Applied Physics Letters* **94** (2009), 223101, DOI: 10.1063/1.3147855.
- [16] O. Turan, N. Chakraborty and R.J. Poole, Laminar Rayleigh-Bénard convection of yield stress fluids in a square enclosure, *Journal of Non-Newtonian Fluid Mechanics* **171-172** (2012), 83 – 96, DOI: 10.1016/j.jnnfm.2012.01.006.
- [17] B.L. Xu, Q. Wang, Z.H. Wan, R. Yan and D.J. Sun, Heat transport enhancement and scaling law transition in two-dimensional Rayleigh-Bénard convection with rectangular-type roughness, *International Journal of Heat and Mass Transfer* **121** (2018), 872 – 883, DOI: 10.1016/j.ijheatmasstransfer.2018.01.051.

